

**Inhomogeneous Dislocation Distributions and the Formation of Dislocation Cell Structure**

In his paper Holt [1] pointed out that, by analogy with the spinodal decomposition of a supersaturated solid solution, a statistical distribution of parallel screw dislocations with uniform density  $\rho_0$  is unstable. In order to minimise the total elastic energy an inhomogeneous distribution with a non-uniformly modulated dislocation density is formed. This results ultimately in the formation of a more or less cellular dislocation structure. The cell diameter  $d$  is of the order of the wavelength  $\lambda$  of the density modulation and is proportional to  $\rho_0^{-1/2}$

$$d \simeq \lambda \simeq K\rho_0^{-1/2}, \tag{1}$$

where  $K$  is a constant.

The purpose of this paper is to test Holt's formula (equation 1) experimentally by means of precise etch pit measurements on LiF single

crystals and to contribute further data on the relation between cell diameter and mean screw dislocation density.

Highly pure and Mg-doped  $\langle 100 \rangle$  oriented LiF single crystals have been compressed in creep tests at temperatures  $375^\circ \leq T \leq 800^\circ\text{C}$  and stresses  $0.06 \leq \sigma \leq 3.50 \text{ kp/mm}^2$ . In order to investigate the dislocation structure, deformation was discontinued in the steady state of deformation (secondary creep range) at strains  $\geq 0.4$  (see below). After rapid cooling to room temperature under load the samples were etched on a (100)-cross section in the middle part of the sample. Because of the  $\langle 100 \rangle$ -specimen orientation and  $\langle 110 \rangle \{110\}$  glide geometry only screw dislocations were etched and counted. To test equation 1 the average dislocation density  $\rho_0$  in cm per cm<sup>3</sup> was determined rather than the local dislocation density. Various values of  $\rho_0$  and  $d$  were obtained by variation of  $\sigma$  and  $T$ . The mean cell diameter  $d$  was determined by the method of Smith and Guthman [2]. For further

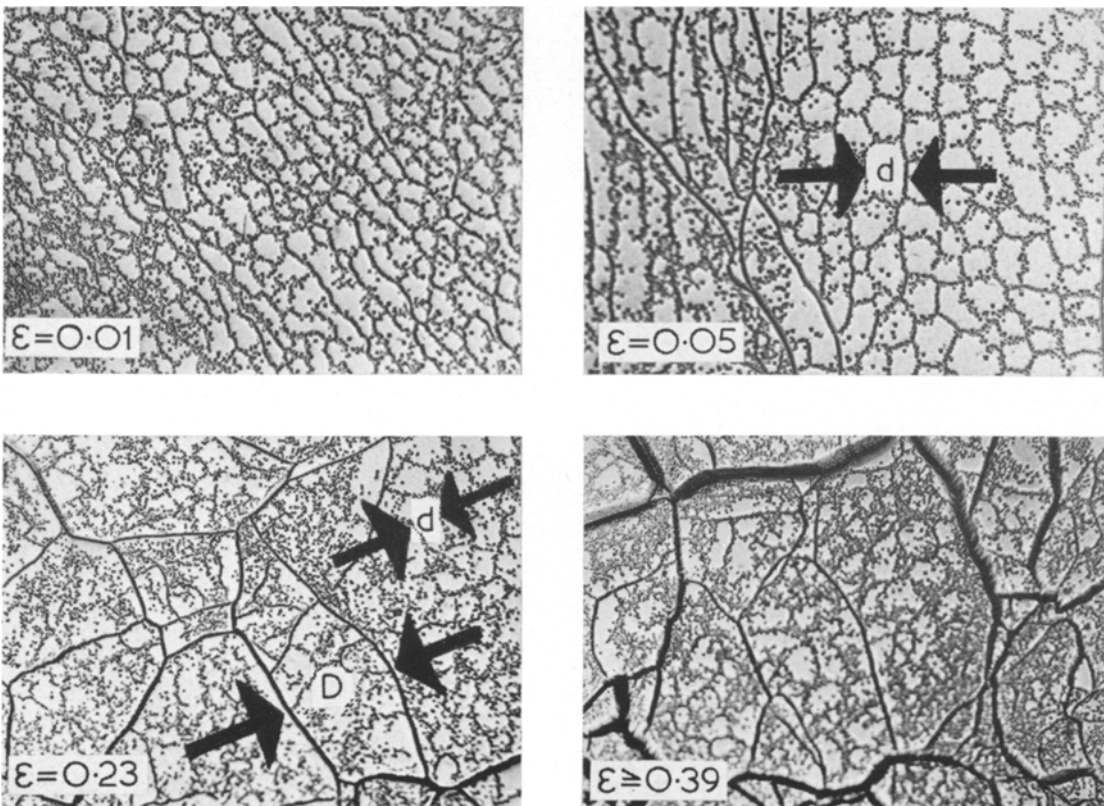


Figure 1 Dislocation cell structure in a LiF single crystal crept at  $T = 500^\circ\text{C}$  and  $\sigma = 0.6 \text{ kp mm}^{-2}$  after various strains. The two types of boundaries are seen, mean spacings  $D$  and  $d$  respectively. Etching on a (100)-cross-section ( $200\times$ ).

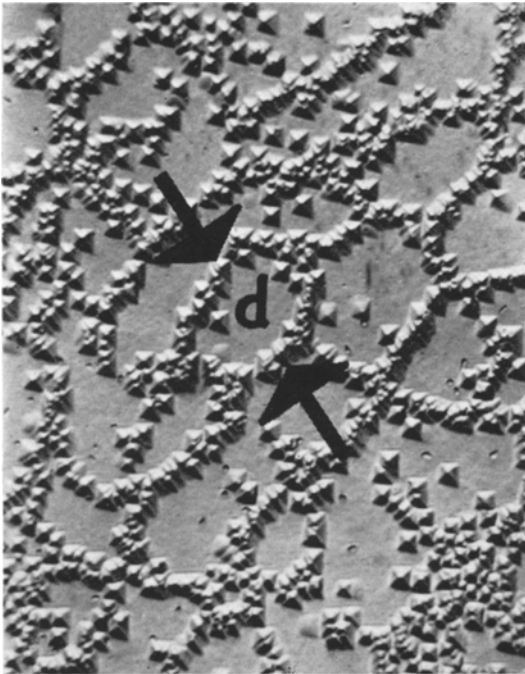


Figure 2 Clustering of dislocations into cell walls (low angle subgrain boundaries) with spacing  $d$ . Sample was crept at  $T = 500^\circ\text{C}$ ,  $\sigma = 0.6 \text{ kp mm}^{-2}$  ( $1000\times$ ).

experimental details see [3, 4]. In fig. 1 the observed dislocation structure after various creep strains is shown. From the beginning of deformation the dislocations are arranged in cells and neither statistically distributed nor arranged in glide bands. Two types of cell boundaries are observed; following Hasegawa and coworkers [5] we call these (figs. 1, 2):

high angle subgrain boundaries, mean separation  $D$ ,

low angle subgrain boundaries or cells, mean diameter  $d$ .

After a transient stage ( $\epsilon < 0.4$ ) an equilibrium structure is formed: the dislocation density and the cell diameters of both boundary types remain constant with respect to strain and time. When, at constant creep stress, the deformation rate  $\dot{\epsilon}$  reaches a constant value ("steady state deformation rate") this structure is called "steady state dislocation structure". The dependence of the steady state parameters  $\dot{\epsilon}$ ,  $D$ ,  $d$  and  $\rho_0$  on temperature, stress, pre-deformation, doping level etc. and their role in the high-temperature deformation will be reported elsewhere [3]. Here we will merely consider the correlation between the mean steady state cell diameter  $d$  of low angle

subgrain boundaries and the mean dislocation density  $\rho_0$ .

In fig. 3 the cell diameter is plotted versus reciprocal square root of the dislocation density. The measured  $d$ -values (or in other terms the wavelengths of density modulation) lie in the range 1-100  $\mu\text{m}$ . The data points are well fitted by a straight line through the origin with a slope

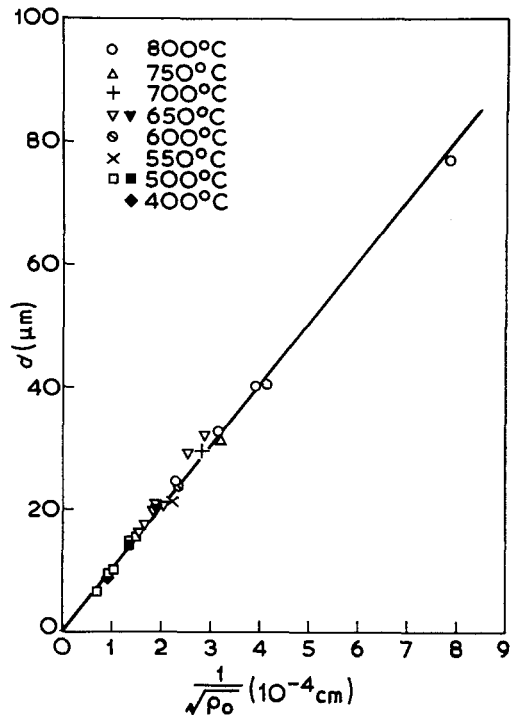


Figure 3 Relation between mean cell diameter  $d$  and average dislocation density  $\rho_0$ . Open symbols represent data points obtained from high purity LiF specimens, full symbols represent data points obtained from specimens with 1110 ppm Mg.

$K = 10$ , and are independent of temperatures and Mg-doping level.

This result is significant because two assumptions of the model are not fulfilled here: Holt treated an idealised dislocation array consisting of parallel screw dislocations. On the other hand, it is often observed that cell boundaries are established by dislocations with mainly edge character [6, 7, 8]. Furthermore, the cell networks in LiF often consist predominantly of edge dislocations. Also, Holt supposed that equation 1 would not apply if the dislocation mobility is high enough, which is certainly the case at the high temperatures applied in the present

investigation, so that annihilation and other recombination reactions occur and specifically low energy boundaries would be expected. This restriction seems not incisive in the present case for the following reason: Holt treated the rearrangement of a statistical distribution of dislocations into a modulated distribution assuming the total number of dislocations to be constant with respect to time. In fact this condition is fulfilled for LiF even in the steady state of deformation [3], which is characterised by a dynamic equilibrium between work hardening processes and recovery processes. Thus the rate of dislocation generation is balanced by the rate of dislocation annihilation. Therefore we feel that steady state values of  $\rho_0$  and  $d$  are particularly suitable to verify equation 1.

### Conclusion

Holt's model gives an excellent contribution to the basic understanding of cell formation. The good agreement between experimental data and Holt's equation 1 shows that this formula describes very well the modulated dislocation configuration observed in LiF at high temperatures during steady state deformation.

### Acknowledgements

The author wishes to thank Professor B. Ilschner and Dr. W. Blum for helpful comments on the manuscript and Mr. G. Streb for the deformation measurements and etch pitting.

### References

1. D. L. HOLT, *J. Appl. Phys.* **8** (1970) 3197.
2. C. S. SMITH, L. GUTHMAN, *Trans. AIME* **197** (1953) 81.
3. B. REPPICH, G. STREB, to be published.
4. G. STREB, Diploma Thesis, Univ. Erlangen-Nürnberg (1971).
5. T. HASEGAWA, H. SATO, S. KARASHIMA, *Trans. Jap. Inst. Met.* **11** (1970) 4.
6. A. H. CLAUSER, B. A. WILCOX, J. P. HIRTH, *Acta Met.* **18** (1970) 381.
7. A. ORLOVA, J. CADEK, *Phil. Mag.* **21** (1970) 509.
8. A. SEEGER, M. WILKENS, in "Reinstoffprobleme III, Realstruktur und Eigenschaften von Reinstoffen." (Akademie-Verlag, Berlin, 1967) p. 29.

Received and accepted  
29 December 1970

B. REPPICH  
Institut für  
Werkstoffwissenschaften I  
Universität Erlangen-Nürnberg,  
Germany

### *Nematic to Smectic Transition in Linear Polyethylene*

Lupolen 6001 H (BASF, Germany) was stretched ten-fold at 80°C from a neck which in a special oven had a length of only 2 mm. Both density  $\rho$  and the long periodicity  $P$  increase in a well-known manner by annealing at temperatures higher than 110°C in a first period of some minutes. Then suddenly  $\rho$  stays constant over a second period of some minutes while  $P$  solely increases [1]. From a careful two-dimensional analysis of small angle X-ray scattering by means of the theory of paracrystals, one can prove that during the second period the nematic-like superstructure with chains, regularly folded at the crystalline amorphous interfaces, turns into a smectic-like superstructure with quite irregularly folded chains. The interface now is rough in the chain direction with a continuous transition zone, between crystalline and amorphous regions, of about 30 Å length. The NMR

spectrum in the first period shows an increasing second moment  $\langle H_x^2 \rangle$  of the crystalline component [2]. During the second period the second moment suddenly decreases. This, in connection with the constant  $\rho$ , proves that during the second period the chains in the crystalline domain regain a higher mobility without enlarging the volume of the "crystalline phase". As a consequence of this the observed change of the structure of the interfaces can take place. At the end of the second period  $\rho$  together with  $P$  begins to increase again with annealing time. Now many crystalline parts of adjacent ultrafibrils are aligned parallel to each other, building up thicker ultrafibrils with diameters of about 200, 300, 400 Å and more.

The folding positions of the molecules within these domains also align increasingly during the next minutes. Then the interfaces again become as smooth as at the end of the first period.

From the above mentioned two-dimensional small angle analysis it can be proved that the